


Review

High-Pressure Polymorphism in Hydrogen-Bonded Crystals: A Concise Review

Tingting Yan ^{1,*} , Dongyang Xi ², Qiuxue Fang ¹, Ye Zhang ³, Junhai Wang ¹ and Xiaodan Wang ²

¹ School of Science, Shenyang Jianzhu University, Shenyang 110168, China; fqixue@sjzu.edu.cn (Q.F.); jhwang@sjzu.edu.cn (J.W.)

² School of Materials Science and Engineering, Shenyang Jianzhu University, Shenyang 110168, China; xidy12@sjzu.edu.cn (D.X.); happywxd0402@sjzu.edu.cn (X.W.)

³ School of Civil Engineering, Shenyang Jianzhu University, Shenyang 110168, China; zy02470@sjzu.edu.cn

* Correspondence: yanтт@sjzu.edu.cn; Tel.: +86-136-2406-3066

Abstract: High-pressure polymorphism is a developing interdisciplinary field. Pressure up to 20 GPa is a powerful thermodynamic parameter for the study and fabrication of hydrogen-bonded polymorphic systems. This review describes how pressure can be used to explore polymorphism and surveys the reports on examples of compounds that our group has studied at high pressures. Such studies have provided insight into the nature of structure–property relationships, which will enable crystal engineering to design crystals with desired architectures through hydrogen-bonded networks. Experimental methods are also briefly surveyed, along with two methods that have proven to be very helpful in the analysis of high-pressure polymorphs, namely, the ab initio pseudopotential plane-wave density functional method and using Hirshfeld surfaces to construct a graphical overview of intermolecular interactions.

Keywords: high pressure; diamond anvil cell; polymorphism; hydrogen bonds



Citation: Yan, T.; Xi, D.; Fang, Q.; Zhang, Y.; Wang, J.; Wang, X. High-Pressure Polymorphism in Hydrogen-Bonded Crystals: A Concise Review. *Crystals* **2022**, *12*, 739. <https://doi.org/10.3390/cryst12050739>

Academic Editors: Jingxiang Yang, Xin Huang and Borislav Angelov

Received: 15 April 2022

Accepted: 18 May 2022

Published: 20 May 2022

Publisher's Note: MDPI stays neutral with regard to jurisdictional claims in published maps and institutional affiliations.



Copyright: © 2022 by the authors. Licensee MDPI, Basel, Switzerland. This article is an open access article distributed under the terms and conditions of the Creative Commons Attribution (CC BY) license (<https://creativecommons.org/licenses/by/4.0/>).

1. Introduction

Polymorphism (Greek: poly = many, morph = form) is a term applied in several areas to describe the diversity of nature.

Mitscherlich (1822, 1823) is generally regarded as the first person to apply polymorphism to crystallography when he recognized various crystal structures of the same compound in several arsenates and phosphate salts. Polymorphism, like many other words in chemistry, lacks a comprehensive definition. McCrone (1965) addresses this issue, and his working definition of polymorphism and the attached stipulations are still as influential as they were when he initially enunciated them.

A polymorph, according to McCrone, is “a solid crystalline phase of a particular compound that results from the possibility of at least two distinct configurations of that compound’s molecules in the solid form”.

Solid forms of the same compound exhibit different physicochemical properties, such as melting point, boiling point, hardness, and conductivity [1–3]. These features are crucial in a wide range of industrial and commercial applications [4–7]. Given the multiple ways in which a new polymorph is innovative, it is vital to characterize and regulate its polymorphic behavior during its development and marketing. Drug goods, particularly in the pharmaceutical business, undergo various manufacturing processes before they reach the market [8–10]. A pharmaceutically active molecule’s chemical structure affects its activity and toxicity [11–14]. Thus, understanding the structural stability of polymorphs is crucial to physics, chemistry, and pharmaceuticals.

High pressure has been shown to be a powerful approach for investigating polymorphism [15–21]. Multitudinous new high-pressure polymorphs related to simple molecules

(e.g., alcohols and carboxylic acids), more complex systems (e.g., amino acids), and substantially larger systems (e.g., energetic materials, pharmaceuticals, metal organic frameworks, and transition metal complexes) have been produced [22–32].

Under identical high-pressure circumstances, the orthorhombic and monoclinic polymorphs of L-cysteine are affected differentially. Although the two L-cysteine polymorphs coexisting under environmental conditions have different density values, increasing the pressure does not change the orthorhombic polymorph with lower density into the monoclinic polymorph with higher density. On the contrary, each of the two polymorphs has undergone its own series of structural changes and has become a unique set of high-pressure phases. The irreversibility of the phase transition in the orthorhombic polymorphs of L-cysteine and the formation of new phases during decompression or the second compression cycle illustrate the kinetic control of pressure-induced phase transitions in crystalline amino acids [33]. Glycine is a classic case study in high-pressure polymorphism research. The α -form of glycine is stable to 23 GPa, the β -form undergoes phase transition to a new form at 0.76 GPa, and the γ -phase transforms into the ϵ -phase at 2 GPa [34–37]. Two paracetamol polymorphs are studied to determine the importance of hydrogen bonding and crystal structure. At 443 K, paracetamol changes from form-III to form-I with a compression of 0.2 GPa [38,39]. Therefore, it is concluded that pressure has an unmatched function to modify crystal structures, especially during phase transitions or the formation of new polymorphs.

Due to its directionality, reversibility, and saturability, hydrogen bonding, as an important intermolecular interaction, plays a vital role in polymorphism [40–43]. Pressure has a long history of decreasing the intermolecular gap between materials and bringing atoms closer together. This feature illustrates that pressure can alter the strength of hydrogen bonding [44]. Increased pressure has been shown to strengthen weak and moderate D–H...A connections (where D and A denote a donor and acceptor, respectively), resulting in a lengthened D–H distance. By contrast, pressure has little effect on strong hydrogen bonding [45,46]. Pressure-induced changes in hydrogen bonding can also result in changes in crystal symmetry, most frequently in conjunction with the effects of π -stacking, van der Waals, and electrostatic interactions. Thus, the cooperativity of various noncovalent interactions and changes in hydrogen bonds as a function of pressure are crucial for material structural stability [4–50].

Extensive research has been conducted on hydrogen-bonded polymorphs under high pressures, particularly for diamond anvil cell (DAC) methods. Compressive strength, hardness, and transparency to visible light are not the only properties of diamond that make it such a good choice for anvils. Diamond is also extraordinarily transparent to parts of the electromagnetic spectrum that are invisible. Many kinds of in situ characterizations based on the DAC, including Raman scattering, infrared, angle-dispersive X-ray diffraction (ADXRD), UV absorption, and fluorescence spectroscopy, have gathered significant information about pressure-induced changes in intermolecular interactions. In researching polymorphic systems, these high-pressure techniques provide considerable precision, accuracy, and sensitivity. These polymorphic materials have demonstrated a variety of critical functions and properties [51–56].

High-pressure science was dominated by hydraulically powered anvil and piston-cylinder devices from the early 1900s to the 1960s. These machines are monstrous in size and require the operation of specialized laboratories. As the gasketed DAC developed in the mid-1960s, high-pressure research technology became less demanding [57,58]. As shown in Figure 1, the DAC's basic concept is as uncomplicated as previously described [59]. Samples are placed in the metal gasket hole between the flat and parallel culets of two diamond anvils. The sample sustains high pressure when an external force pushes the two opposed anvils together. By filling the pressure chamber with a liquid pressure-transmitting substance, hydrostatic pressure conditions can be achieved [60,61]. A well-calibrated ruby fluorescence pressure scale is used to determine the pressure within the DAC sample chamber.

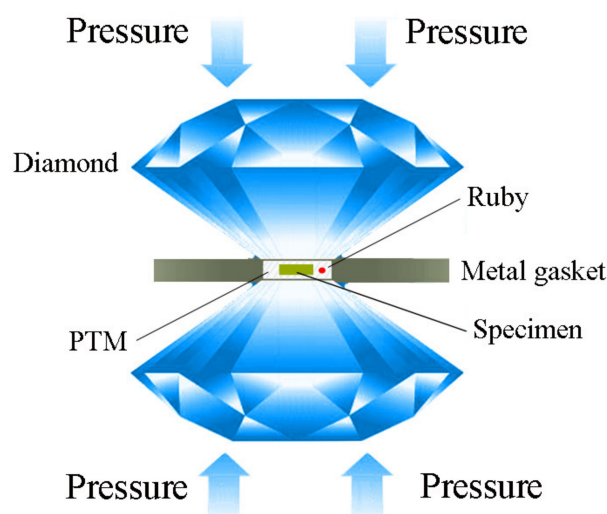


Figure 1. Schematic of DAC for high-pressure studies.

This review outlines recent advances in polymorphism in hydrogen-bonded crystals produced by the application of in situ high-pressure techniques and briefly discusses new development challenges. Additionally, potential obstacles and future directions are evaluated.

2. High-Pressure Polymorphism in Amides

Amides are particularly important because they are abundant in nature and are commonly employed in industry and technology as structural materials. In addition, the hydrogen bonds within the functional group of amides exhibit a similar directionality to those found in carboxylic acid synthons.

As a first-line antituberculosis medicine, pyrazinamide ($C_5H_5N_3O$, pyrazine-2-carboxamide, PZA) has been included on the World Health Organization's Model List of Essential Medicines. This medication is an infrequent instance of a conformationally stiff molecule with four polymorphs, namely, the α , β , γ , and δ forms [62–64]. Figure 2 illustrates the molecular packings in several polymorphs.

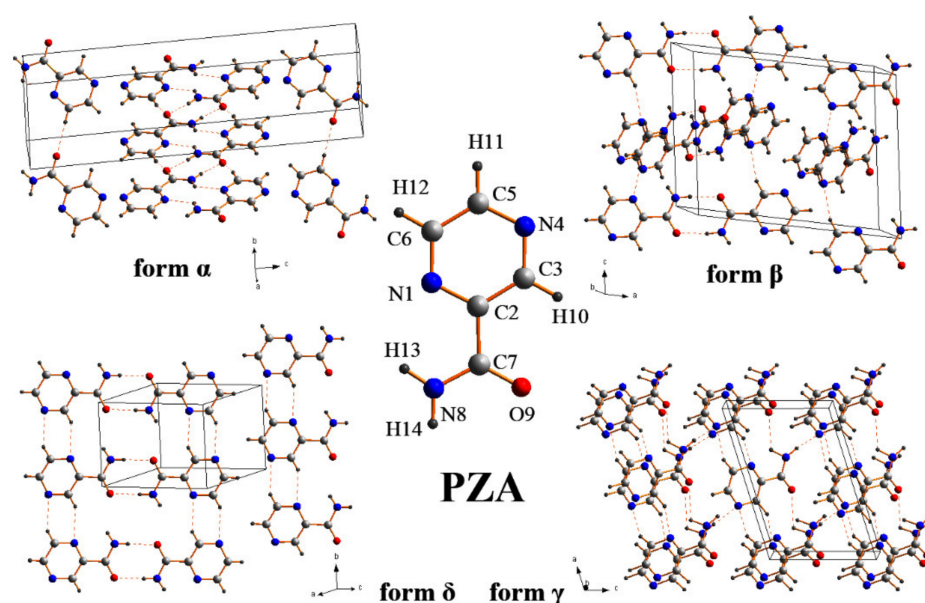


Figure 2. Crystal structures of PZA polymorphic forms: α , β , δ , and γ forms. Reprinted with permission from Ref. [65]. Copyright 2012 American Chemical Society.

The phase interactions between the four polymorphs have been widely researched at ambient pressure. Once the pure δ and γ forms undergo hand-grinding, they will be converted to the α -form in 45 min. The α , β , and δ forms will be converted to the γ -form upon being heated to 165 °C. After being cooled to room temperature, the γ -form can remain stable for up to 6 months before gradually converting to the α -form. In other words, a stable form at a high temperature can be retained at ambient temperature as a metastable form. Within the temperature range of -263 to -13 °C, the α -form changes into the δ -form.

We have adopted the in situ Raman spectroscopy and ADXRD techniques to examine the high-pressure responses of three forms (α , δ , and γ) of PZA [65]. At 4 GPa, the γ -phase transforms to the β -phase, while the other two forms preserve their original structures up to 14 GPa. The volume of the γ -phase is reduced by $\sim 3\%$ at a pressure greater than 4 GPa. The bulk modulus and pressure derivatives for the γ -form are $B_0 = 6.3 \pm 0.4$ GPa and $B_0' = 10.0 \pm 0.3$. These parameters for the β -form are $B_0 = 7.9 \pm 0.3$ GPa and $B_0' = 5.8 \pm 0.2$. These equations imply that the β -form is more difficult to compress, which is consistent with the conclusion of lattice vibration analysis in the Raman spectra.

The β -form cannot be obtained entirely under ambient conditions. It always crystallizes alongside the γ -form. The α - and δ -forms' stability under compression is attributable to their unique dimer link. Previous studies have shown that the dimers are connected by relatively strong N–H \cdots O hydrogen bonds in the α , β , and δ forms, whereas head-to-tail connection is only present in the γ -form through the N–H \cdots N hydrogen bonds [66].

The pressure-induced γ -to- β phase change is exceptional in that it happens between two well-characterized polymorphs and is reversible. Additionally, the phase transition is detected at a wide range of pressures. Hysteresis behavior is very common in high-pressure investigations and is a characteristic of first-order phase transitions. The γ -form is not recovered until the pressure is close to the ambient level, which indicates an energy barrier to the transition [67]. An imbalance between hydrogen bonding and van der Waals interactions within γ -PZA could be responsible for the phase transition. The distances between PZA molecules inside the 3D structure decrease as pressure increases, strengthening hydrogen bonding and increasing overall Gibbs free energy. The free energy of the phase transition is reduced by rotating the PZA molecules and reassembling hydrogen bonds, resulting in a ~ 4 GPa phase transition.

Malonamide ($C_3H_6N_2O_2$) is a model compound for investigating the hydrogen bonding interactions that occur when amides are compressed. This technique is used to manufacture pharmaceuticals and insecticides. This substance is analogous to a glycine residue with the peptide group inverted. Malonamide derivatives are of particular relevance because they are used in the manufacture of peptidomimetic compounds. Malonamide is a polymorphous compound that crystallizes into monoclinic, tetragonal, and orthorhombic crystal forms [68–70]. The unit cell parameters of the monoclinic forms are $a = 15.78(0)$ Å, $b = 4.63(7)$ Å, $c = 9.33(1)$ Å, $\beta = 133.84(0)^\circ$, $V = 492.46(4)$ Å³, and $Z = 4$. Tetragonal forms crystallize into $a = 5.3140(3)$ Å, $c = 15.5360(12)$ Å, $V = 438.71(5)$ Å³, and $Z = 4$. Crystallographic parameters of the orthorhombic forms are $a = 5.3602(9)$ Å, $b = 7.5178(8)$ Å, $c = 11.791(2)$ Å, $V = 475.14(12)$ Å³, and $Z = 4$.

The monoclinic form is chosen as the sample and compressed to a pressure of 10.4 GPa in a DAC at room temperature [71]. In situ Raman spectroscopy is utilized to detect structural changes caused by pressure. At 2.1 GPa, the Raman spectra show considerable changes, indicating the occurrence of a phase transition. At various pressures, the Raman spectrum is analyzed in terms of its fluctuations, which include the elimination of original modes, the development of new modes, and discontinuous changes in the Raman modes' pressure dependence.

Ab initio calculations are adopted to calculate the changes in molecular configurations and hydrogen-bonded networks. The computed results indicate that the molecules distort slightly in reaction to pressure. As a result, the original hydrogen bonds between N–H \cdots O are twisted. Additionally, the hydrogen-bonded patterns shift significantly. All amine groups participate in hydrogen bonding in the ambient structure. Eight hydrogen bonds

are created between each molecule, including four donors and four acceptors. At a pressure of 10 GPa, however, one sort of asymmetric unit molecule establishes six hydrogen bonds with three donors and three acceptors. These findings corroborate the Raman spectra observed in the NH_2 stretching modes. The appearance of NH_2 asymmetric stretching modes indicates that the hydrogen bond networks have been reconstructed. Meanwhile, the modes that are related to $\text{N-H}\cdots\text{O}$ hydrogen bonds, including the NH_2 twisting, NH_2 rocking, NH_2 scissoring, NH_2 bending, CO bending, and CO stretching modes, all vary remarkably during phase transition. These variations indicate that the hydrogen bond donors and acceptors adopt new orientations.

We use Hirshfeld surfaces and fingerprint plots to compare changes in packing patterns and intermolecular interactions (Figure 3). This method simplifies the process of determining hydrogen bonding and van der Waals radius. On Hirshfeld surfaces, blue patches denote long interactions, and red regions denote short contacts. When the pressure is increased, the blue parts shrink, and the red regions expand. This development corresponds to the typical shortening of connections under conditions of high pressure. The two “spikes” reflect $\text{N-H}\cdots\text{O}$ hydrogen bonding in both plots. The upper spike is the hydrogen bond donor (where $d_e > d_i$), whereas the lower spike is the hydrogen bond acceptor (where $d_i > d_e$). This conclusion is evident from the fingerprint plot: the $\text{N-H}\cdots\text{O}$ spikes grow less prominent as the plot moves closer to the origin. The reduced maximum values of d_e between ambient pressure (2.399 Å) and 10 GPa (1.921 Å) are attributable to the overall shortening of the long contacts. The contribution of the $\text{H}\cdots\text{O}$ connections remains stable at 23.9% at ambient pressure and 21.1% at 10 GPa, respectively. The $\text{H}\cdots\text{H}$ contacts are compressed from 2.6 Å at ambient pressure to 2.2 Å at 10 GPa. Moreover, the contribution of the $\text{H}\cdots\text{H}$ interaction changes from 32.3% to 30.2%. According to the computed results, fluctuations in the NH_2 stretching Raman vibrations, and the degree of freedom of the molecules, the phase transition of crystalline malonamide is likely induced by rearrangements of the hydrogen-bonded networks.

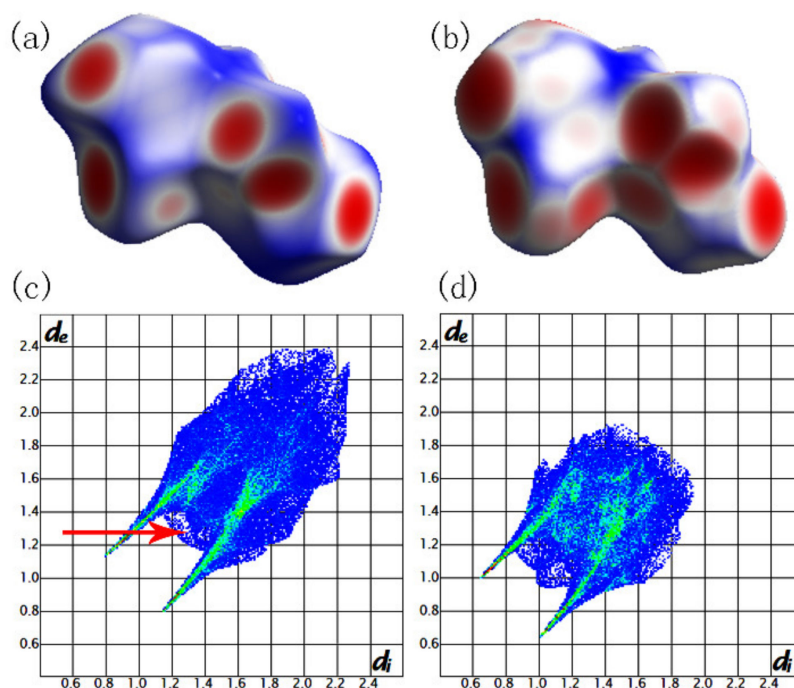


Figure 3. Hirshfeld surfaces mapped with d_{norm} and fingerprint plots for malonamide at ambient pressure (a,c) and at 10 GPa (b,d). Reprinted with permission from Ref. [71]. Copyright 2015 Royal Society of Chemistry.

Acetamide (H_3CCONH_2) is a hydrogen-bonded system with a basic structure that can be used as a model system for researching hydrogen-bonded systems under high pressures. Additionally, since acetamide contains just one peptide link, it can shed light on the structures of complicated peptides and proteins. Acetamide crystallizes into two crystal forms under ambient conditions, namely, the stable rhombohedral space group $R3c$ and the metastable orthorhombic space group $Pccn$ [72,73].

At pressures up to 16 GPa, in situ ADXRD and Raman scattering are utilized to examine the vibrational and structural properties of rhombohedral acetamide [74]. The ambient unit cell is seen in Figure 4a. Each acetamide molecule includes two acceptors and two donors, resulting in the formation of four $\text{N-H}\cdots\text{O}$ hydrogen bonds with other molecules. As a result, the equilibrium between hydrogen bonding and van der Waals interactions has an effect on the acetamide structure's stability under high pressure. At 0.9 GPa and 3.2 GPa, two structural phase transitions are observed, as indicated by significant changes in the Raman spectrum and discontinuities in peak positions vs. pressure. Significant alterations in the ADXRD patterns, as seen in Figure 4b, further verify the phase transition. Pawley refinement is used to determine the lattice parameters of the high-pressure phase-II using ab initio calculations. The crystal structure of phase-II can be indexed and refined as a monoclinic system with a potential $C2/c$ space group; the lattice constants are as follows: $a = 7.34(2) \text{ \AA}$, $b = 17.26(1) \text{ \AA}$, and unit cell volume $V = 690.7(1) \text{ \AA}^3$. Phase-III has similar diffraction patterns to phase-II, implying that the two high-pressure phases may have similar structures.

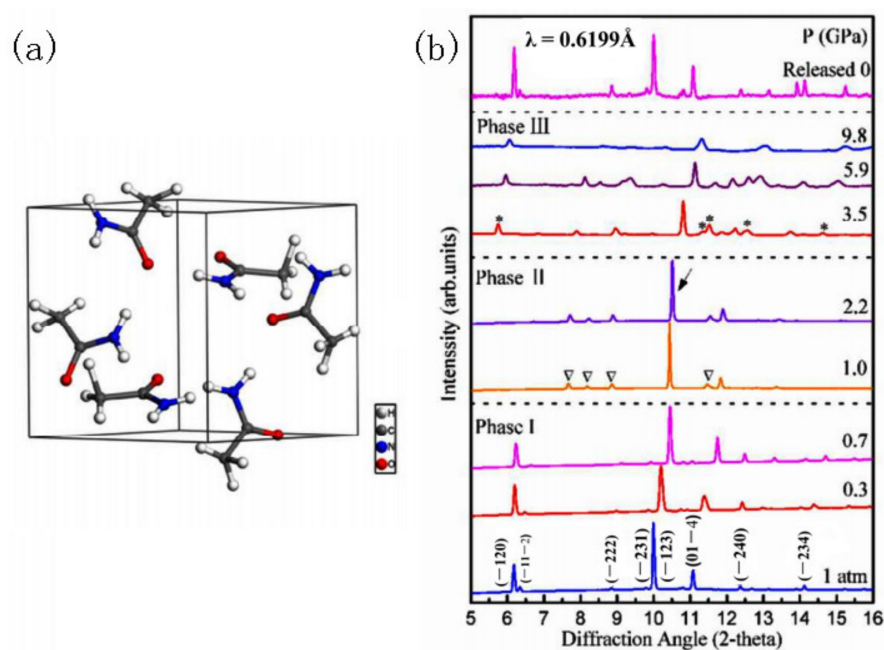


Figure 4. Ambient unit cell (a) and representative ADXRD patterns of acetamide crystal at different pressures (b). The peaks marked by asterisks and hollow triangles indicate the emergences of new phases. Reprinted with permission from Ref. [74] Copyright 2013 Royal Society of Chemistry.

The mechanism for pressure-induced phase changes has been postulated based on experimental and computational studies. Hydrogen bonding and van der Waals forces are the two key interactions that maintain acetamide's structural integrity at ambient temperature. The van der Waals forces between neighboring acetamide molecules increase as pressure increases because the distances between nearby molecules shrink. At the same time, the shorter hydrogen bonds make hydrogen bonding contact easier. The total Gibbs free energy available to the cosmos is enhanced by this method. With further compression, the acetamide crystal structures can no longer support the increasing Gibbs free energy. Thus, acetamide molecules slide and/or rotate, reorganizing hydrogen-bonded networks

(through reconstruction and torsion) to lower the free energy. Thus, acetamide crystals undergo phase changes at various critical pressures (0.9, 3.2 GPa).

3. High-Pressure Polymorphism in Hydrazides

Maleic hydrazide ($C_4H_4N_2O_2$, MH), a well-known plant growth inhibitor in agriculture, comes in three polymorphic forms: triclinic MH1 and monoclinic MH2 and MH3 [75–77]. In their crystal structures, the three polymorphs exhibit identical patterns of hydrogen bonding, namely, an $O-H\cdots O$ motif that connects infinite chains of molecules. These polymorphs are connected into ribbons of double chains through $N-H\cdots O$ interactions.

The pressure-induced polymorphism of MH3 is investigated by in situ ADXRD and high-pressure Raman spectroscopy [78]. At 2 GPa, variations in the Raman spectrum suggest the presence of a pressure-induced phase transition. High-pressure ADXRD tests are carried out to further characterize this transition, as seen in Figure 5a. The monoclinic polymorphic form of MH2 with space group $P2_1/c$ is connected to the pressure-induced phase. The new MH2 phase remains when the pressure is increased even more. Further analysis indicates that this pressure-induced polymorphic transformation could be attributed to changes in the hydrogen-bonded ribbons. The ADXRD pattern indicates that this MH3 to MH2 polymorphism is partially reversible when the sample is returned to atmospheric pressure, with the majority of the sample reverting to the original MH3 structure. The quenched sample contains 68.3 wt% MH3 and 31.7 wt% MH2, according to the Rietveld quantitative phase analysis results in Figure 5b. The coexistence of these two polymorphic forms upon complete pressure release could be explained by their identical hydrogen-bonded aggregates and similar energies.

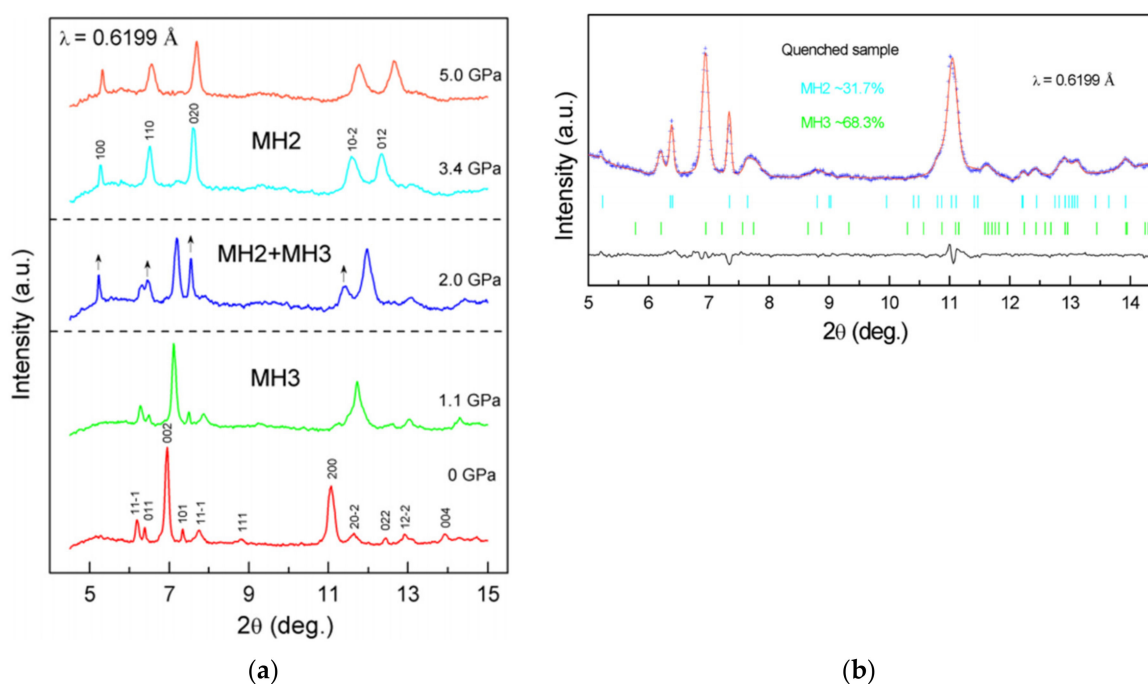


Figure 5. (a) Representative ADXRD patterns at elevated pressures. Arrows indicate new peaks. (b) Quantitative phase analysis based on the Rietveld fit of the diffraction patterns collected from the quenched sample: red line, experimental pattern; blue dotted line, simulated pattern; the black line is the fit residual. Reprinted with permission from Ref. [78]. Copyright 2014 American Chemical Society.

The conformational polymorphism oxalyl dihydrazide [$H_2N-NH-CO-CO-NH-NH_2$, ODH] has five known polymorphs. The ODH molecule is composed of six possible hydrogen-bond donors ($N-H$ bonds of the NH and NH_2 group) and four possible hydrogen-bond acceptors (oxygen atoms in the $C=O$ groups and nitrogen atoms in the

NH₂ groups). Numerous polymorphisms have been found, including α , β , γ , δ , and ϵ [79]. The crystal structures of the ODH polymorphic forms are depicted in Figure 6.

The molecule's N–N–C–C–N–N backbone is planar in all polymorphs and conforms to the trans-trans-trans conformation. The oxygen atoms of the O=C groups and the hydrogen atoms of the NH groups lie within this plane. The pyramidal structure of the NH₂ group indicates that the nitrogen atom has undergone sp³ hybridization, which enhances the nitrogen atom's capacity to act as a hydrogen-bond acceptor. Computational approaches are utilized to determine the energy sequence of the known polymorphs: $\alpha > \epsilon > \gamma > \delta > \beta$ [80,81].

At a pressure of 20 GPa, high-pressure Raman spectroscopy and ADXRD studies of the five types of ODH are carried out [82]. By applying pressure to the original counterparts, five novel forms are identified. Under high pressure, each polymorph yields a new form, resulting in a total of ten polymorphs, with the new forms being α' , β' , γ' , δ' , and ϵ' . The transition pressure points of the five ODH polymorphs are 12.0, 14.0, 11.3, 10.6, and 6.0 GPa for the α , β , γ , δ , and ϵ forms, respectively, as determined by Raman and ADXRD patterns. Under the influence of shear force, the β -form is changed into the α -form. As a result, high-pressure ADXRD experiments on the β -form cannot be carried out. The new forms might be indexed as $P2_1/c$ for α' , $Pmnb$ for γ' , $P2_1/n$ for δ' , and $P-1$ for ϵ' via ab initio calculations. Several hydrogen-bond donors and acceptors, and low-energy conformational changes in NH and NH₂ groups, all play a role in the molecular conformation of ODH, resulting in a variety of crystal polymorphs. The transition pressures of the α , β , γ , and δ forms are all above 10 GPa, while the ϵ -form is changed into the ϵ' -form at about 6 GPa. This is attributable to the fact that the ϵ -form's structure is significantly different from that of the other polymorphs. The ϵ -form has ribbons that generally run perpendicularly to create a grid-like pattern when viewed in projection along the c -axis. The grid-like structure of the form is not as stable under pressure as the other polymorphs' sheet-like parallel ribbon structures. Therefore, the ϵ -form's phase transition takes place at 6 GPa, at least 4 GPa lower than those of the other four forms.

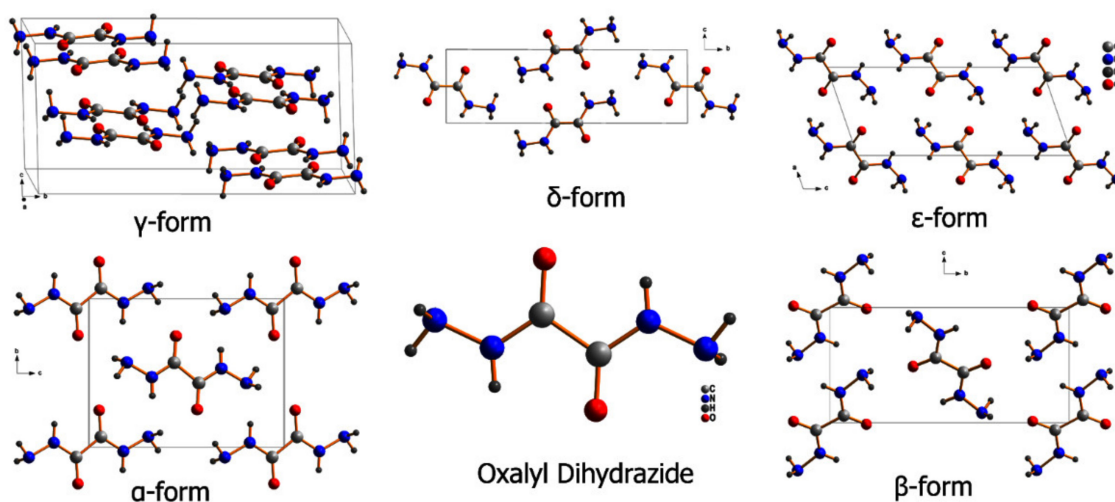


Figure 6. Crystal structures of ODH polymorphic forms: α , β , δ , γ , and ϵ forms. Reprinted with permission from Ref. [82]. Copyright 2015 American Chemical Society.

4. High-Pressure Polymorphism in Carboxylic Acid Derivatives

Because the molecule has distinct functional groups, as do many pharmacological compounds, *p*-aminobenzoic acid (C₇H₇NO₂, PABA) is a practicable substance for the model material. The chemical is largely utilized in the production of medicines. Perfumes, colors, and feedstock additives are some of the other applications. PABA polymorphs have sparked much curiosity among scientists. Two polymorphs are known to exist: the

α - and β -forms. The majority of the reported research on this drug has been focused on crystallography. Jarchow and Banerjee use NMR to confirm the phase transition of α -form crystals at 32 °C [83,84]. When crystallized from a solvent, the transition temperature between the two forms is approximately 25 °C; β -PABA is thermodynamically stable below this temperature [85]. Yang et al. discover that when heated to 96 °C, the β -form can be transformed into the α -form [86].

According to published sources, the two polymorphs are synthesized: the α -polymorph, which is commercially accessible and resembles long, fibrous needles; and the β -polymorph, which resembles prisms. The function of high pressure on the two forms in a DAC is investigated via in situ Raman spectroscopy [87]. Experiments demonstrate that both forms keep their original structures up to a pressure of 13 GPa. For determining the variations in intermolecular interactions, the Hirshfeld surface and fingerprint plot have been applied. Upon a thorough comparison of the small structural alterations and anisotropic properties, we find that the particular dimer link is a factor in maintaining the stability of α -form crystals, while the presence of hydrogen-bonded networks with a four-membered ring structure is a factor in maintaining the stability of the β -form. For α -PABA, the molecular pairs are connected via two O–H \cdots O bonds; a hydrogen-bonded bridge is formed between the two molecules. This bridge resists the effect of pressure along the direction of hydrogen bonds. This visualization is analogous to the behaviors of the α - and δ -forms in pyrazinamide polymorphs. In the tetramer structure of β -PABA, the special four-membered hydrogen-bonded networks can easily twist to release the increased intermolecular interactions, as well as maintain the balance of hydrogen bonding and van der Waals interactions; the structural stability is maintained. The crystal structures of α -PABA and β -PABA under ambient conditions are shown in Figure 7.

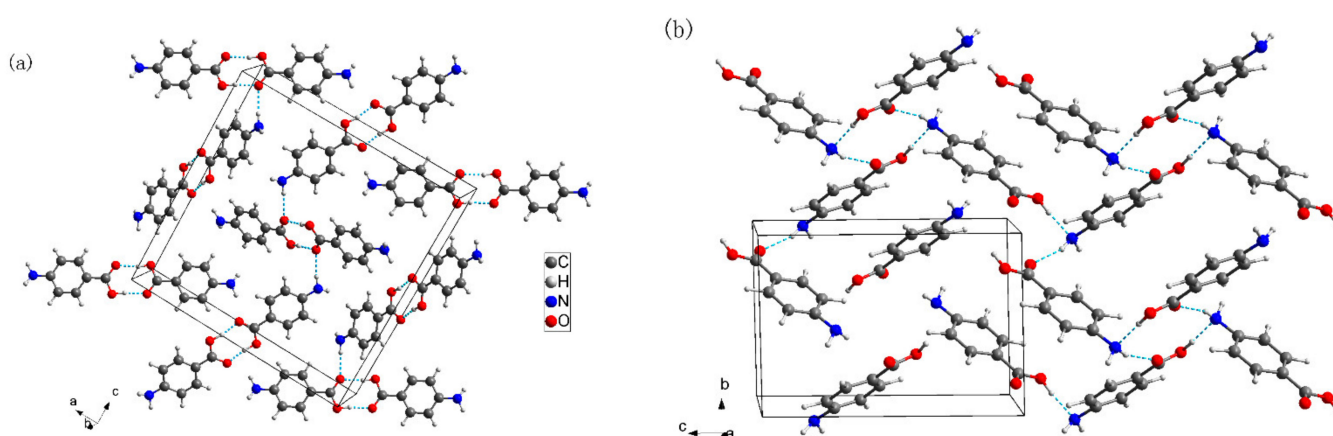


Figure 7. Crystal structures of (a) α -PABA and (b) β -PABA under ambient conditions: the hydrogen bonds are marked as dashed lines. Reprinted with permission from Ref. [87]. Copyright 2014 Royal Society of Chemistry.

Chemists and biologists have always been interested in cinchomeric acid (CA; pyridine-3,4-dicarboxylic acid; $C_7H_5NO_4$) due to its unique structure and characteristics [88–92]. CA is commonly employed in the building of coordination networks due to the flexibility of its metal coordination modes [93,94]. Since 1971, the PDF-2 has been reported to include two CA polymorphs. Form-I and form-II can be prepared concomitantly from the recrystallization of form-II in ethanol/water solution at ambient conditions. A slurry conversion experiment converts form-II to form-I, which will disintegrate before melting, with the form-I melting at 263 °C and form-II melting at 259 °C.

The compression behavior of the two forms is investigated using DACs in conjunction with Raman spectroscopy and ADXRD [95,96]. Once a phase change is produced as the form-I is compressed to about 6.5 GPa, the new polymorph form-III is produced. The ADXRD pattern indicates that this polymorphic transition is partially reversible when the

sample is brought back to ambient pressure, with a portion of the sample reverting to its original form-I structure (Figure 8a). The Raman spectra's lattices and internal modes are evaluated to determine the alterations to the CA form-I molecules' local environment. A low-symmetry triclinic structure with space group $P1$ is shaped by the indexing and refinement of form-III. In CA form-I, the phase transition may be triggered due to the reconstruction of the hydrogen-bonded networks.

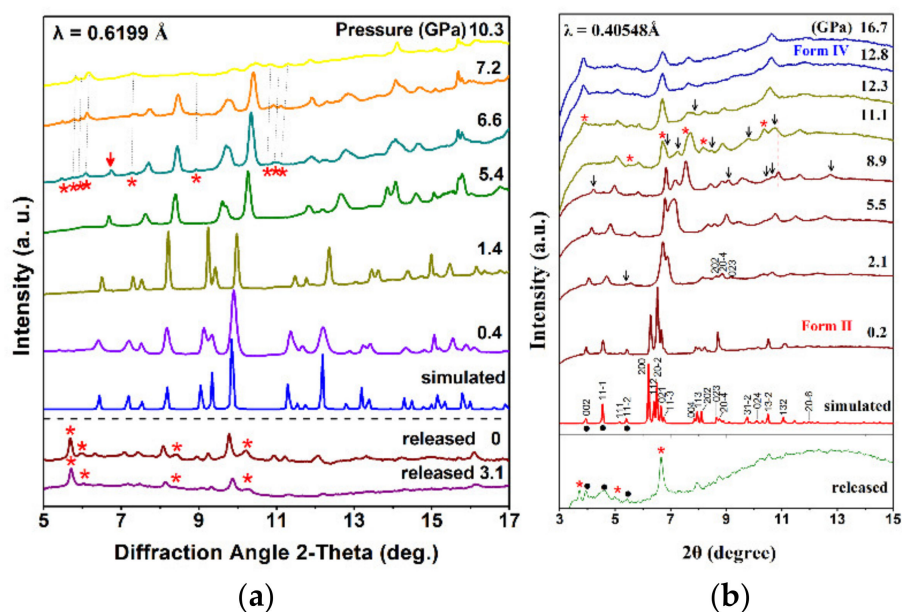


Figure 8. (a) Representative high-pressure ADXRD patterns of CA form-I. Red asterisks indicate new peaks. Down arrow indicates the disappearing diffraction peak. Reprinted with permission from Ref. [95]. Copyright 2019 Institute of Physics (b) Representative high-pressure ADXRD patterns of CA form-II. Red asterisks represent the peaks of form IV. Black dots show the peaks of form II. Down arrows show the disappearing diffraction peaks of form II. Reprinted with permission from Ref. [96]. Copyright 2021 American Chemical Society.

At ~11–13 GPa, a polymorphic transition is visible in the Raman spectra and ADXRD patterns of form-II. From form-II, a new CA polymorph named form-IV is formed. Form-IV could be a monoclinic structure with the space group $P2_1/c$, according to ab initio calculations. In the released ADXRD pattern, as shown in Figure 8b, form-IV peaks coexist with form-II peaks. The reconstruction of hydrogen-bonded networks is the most likely cause of the polymorphic transformation in both experimental and theoretical data.

Phenyl carbamate ($C_7H_7NO_2$, PC) is a widely used pharmaceutical intermediate with a wide range of pharmacological characteristics and uses. Three pure PC polymorphs have been discovered via traditional crystallization methods: form-I, form-II, and form-III. Methanol and acetonitrile are used to crystallize form-I, while ethyl acetate is used to crystallize form-II. At 25 °C, solution-mediated phase transition and solid-state phase transition produce form-I. The computed phenotype-II is 4.6% denser than phenotype-I, according to the Burgers density rule. Changes in HSM, PXRD, and DSC spectra are used to track the development of form-III.

PC form-I has been used to investigate the pressure-induced polymorphic transition and disorder in the amorphous state in polymorphic molecular systems [97]. Under high pressure, no polymorphic transition from crystalline PC-I to type-II crystals can be observed. At a pressure of 12.7 GPa, the evolution of the ADXRD and Raman spectra suggest that a reversible pressure-induced amorphization (PIA) occurs in PC type-I. The ADXRD patterns and diffraction patterns of PC form-I under different pressures are presented in Figure 9. The modifications of PC-I hydrogen bond networks and molecular configuration under pressure are computed by ab initio approach. Hirshfeld surfaces and fingerprint plots are

utilized to rapidly compare changes in packing patterns and intermolecular interactions. Based on experimental and theoretical data, we predict that the PIA of crystalline PC form-I is driven by competition between close packing and long-range ordering. This competition results in the collapse of the hydrogen bonds.

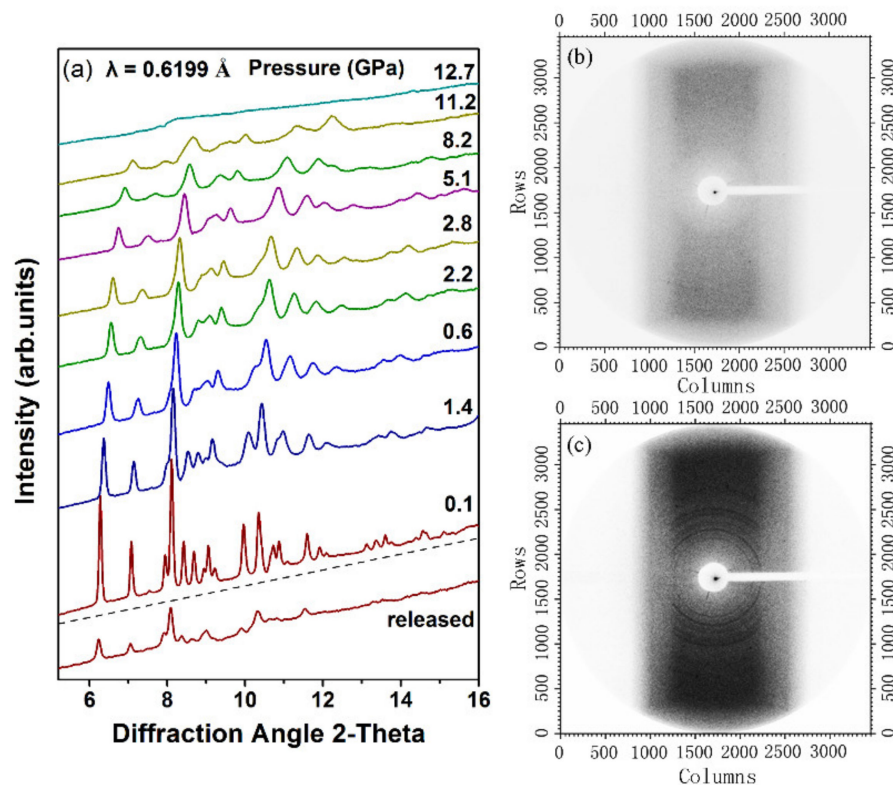


Figure 9. Synchrotron XRD patterns of PC form-I under different pressures (a). Diffraction images of PC form-I compressed under 12.7 GPa (b) and decompressed under ambient pressure (c). Reprinted with permission from Ref. [97]. Copyright 2017 American Chemical Society.

5. Summary

In this review, we have aimed to summarize some of the studies of our group on high-pressure polymorphism in hydrogen-bonded crystals. These crystals are divided into three categories, namely, amides, hydrazides, and carboxylic acid derivatives. These studies have shown that pressure can induce amorphization, the formation of new polymorphs, and phase transitions between different polymorphs. Experimental and computational results have revealed that pressure-induced structural distortions and structural stability can be correlated with the hydrogen bonding.

High-pressure polymorphism is a growing and rapidly expanding scientific topic with a promising future. Hydrogen-bonded crystal research will continue to evolve and improve as new discoveries in powder diffraction, high-pressure crystal formation from solution, and theoretical techniques are established (e.g., density functional theory and crystal structure prediction). Although several fundamental issues remain unsolved, significant progress is being made in several laboratories. However, more research still needs to be done by professionals using high pressures.

Author Contributions: Conceptualization, X.W.; investigation, J.W.; Writing—original draft preparation, Q.F. and Y.Z.; writing—review and editing, T.Y. and D.X. All authors have read and agreed to the published version of the manuscript.

Funding: This review was funded by the National Natural Science Foundation of China, grant numbers 11604224 and 51805336, and Liaoning Provincial Department of Education, grant number LJKZ0596.

Institutional Review Board Statement: Not applicable.

Informed Consent Statement: Not applicable.

Data Availability Statement: Not applicable.

Conflicts of Interest: The authors declare no conflict of interest.

References

1. Cruz-Cabeza, A.J.; Bernstein, J. Conformational Polymorphism. *Chem. Rev.* **2014**, *114*, 2170–2191. [[CrossRef](#)] [[PubMed](#)]
2. Johnstone, R.D.; Lennie, A.R.; Parker, S.F.; Parsons, S.; Pidcock, E.; Richardson, P.R.; Warren, J.E.; Wood, P.A. High-Pressure Polymorphism in Salicylamide. *CrystEngComm* **2010**, *12*, 1065–1078. [[CrossRef](#)]
3. Bond, A.D. Polymorphism in Molecular Crystals. *Curr. Opin. Solid State Mater. Sci.* **2009**, *13*, 91–97. [[CrossRef](#)]
4. Price, C.P.; Grzesiak, A.L.; Matzger, A.J. Crystalline Polymorph Selection and Discovery with Polymer Heteronuclei. *J. Am. Chem. Soc.* **2005**, *127*, 5512–5517. [[CrossRef](#)] [[PubMed](#)]
5. David, W.I.F.; Shankland, K.; Pulham, C.R.; Blagden, N.; Davey, R.J.; Song, M. Polymorphism in Benzamide. *Angew. Chem.* **2005**, *117*, 7194–7197. [[CrossRef](#)]
6. Gavezzotti, A.; Filippini, G. Polymorphic Forms of Organic Crystals at Room Conditions: Thermodynamic and Structural Implications. *J. Am. Chem. Soc.* **1995**, *117*, 12299–12305. [[CrossRef](#)]
7. Nangia, A. Conformational Polymorphism in Organic Crystals. *Acc. Chem. Res.* **2008**, *41*, 595–604. [[CrossRef](#)]
8. Halebian, J.; McCrone, W. Pharmaceutical Applications of Polymorphism. *J. Pharm. Sci.* **1969**, *58*, 911–929. [[CrossRef](#)]
9. Feng, Y.; Hao, H.; Chen, Y.; Wang, N.; Wang, T.; Huang, X. Enhancement of Crystallization Process of the Organic Pharmaceutical Molecules through High Pressure. *Crystals* **2022**, *12*, 432. [[CrossRef](#)]
10. Ali, I.; Tang, J.; Han, Y.; Wei, Z.; Zhang, Y.; Li, J. A Solid-Solid Phase Transformation of Triclabendazole at High Pressures. *Crystals* **2022**, *12*, 300. [[CrossRef](#)]
11. Porter, W.W., III; Elie, S.C.; Matzger, A.J. Polymorphism in Carbamazepine Cocrystals. *Cryst. Growth Des.* **2008**, *8*, 14–16. [[CrossRef](#)] [[PubMed](#)]
12. Nauha, E.; Saxell, H.; Nissinen, M.; Kolehmainen, E.; Schäfer, A.; Schlecker, R. Polymorphism and Versatile Solvate Formation of Thiophanate-Methyl. *CrystEngComm* **2009**, *11*, 2536–2547. [[CrossRef](#)]
13. Bond, A.D.; Boese, R.; Desiraju, G.R. On the Polymorphism of Aspirin. *Angew. Chem. Int. Ed.* **2007**, *46*, 615–617. [[CrossRef](#)] [[PubMed](#)]
14. Nath, N.K.; Kumar, S.S.; Nangia, A. Neutral and Zwitterionic Polymorphs of 2-(p-tolylamino) Nicotinic Acid. *Cryst. Growth Des.* **2011**, *11*, 4594–4605. [[CrossRef](#)]
15. Yu, L. Polymorphism in Molecular Solids: An Extraordinary System of Red, Orange, and Yellow Crystals. *Acc. Chem. Res.* **2010**, *43*, 1257–1266. [[CrossRef](#)]
16. Wilding, M.C.; Wilson, M.; McMillan, P.F. Structural Studies and Polymorphism in Amorphous Solids and Liquids at High Pressure. *Chem. Soc. Rev.* **2006**, *35*, 964–986. [[CrossRef](#)]
17. Carvalho, P.H.B.; Mace, A.; Nangoi, I.M.; Leitão, A.A.; Tulk, C.A.; Molaison, J.J.; Andersson, O.; Lyubartsev, A.P.; Häussermann, U. Exploring High-Pressure Transformations in Low-Z (H₂, Ne) Hydrates at Low Temperatures. *Crystals* **2021**, *12*, 9. [[CrossRef](#)]
18. Daniel, I.; Oger, P.; Winter, R. Origins of Life and Biochemistry under High-Pressure Conditions. *Chem. Soc. Rev.* **2006**, *35*, 858–875. [[CrossRef](#)]
19. Chen, S.; Guzei, I.A.; Yu, L. New Polymorphs of ROY and New Record for Coexisting Polymorphs of Solved Structures. *J. Am. Chem. Soc.* **2005**, *127*, 9881–9885. [[CrossRef](#)]
20. Vasileiadis, M.; Pantelides, C.C.; Adjiman, C.S. Prediction of the Crystal Structures of Axitinib, a Polymorphic Pharmaceutical Molecule. *Chem. Eng. Sci.* **2015**, *121*, 60–76. [[CrossRef](#)]
21. Fabbiani, F.P.; Allan, D.R.; David, W.I.; Moggach, S.A.; Parsons, S.; Pulham, C.R. High-Pressure Recrystallisation—A Route to New Polymorphs and Solvates. *CrystEngComm* **2004**, *6*, 504–511. [[CrossRef](#)]
22. Fabbiani, F.P.A.; Pulham, C.R. High-Pressure Studies of Pharmaceutical Compounds and Energetic Materials. *Chem. Soc. Rev.* **2006**, *35*, 932–942. [[CrossRef](#)] [[PubMed](#)]
23. Laniel, D.; Downie, L.E.; Smith, J.S.; Savard, D.; Murugesu, M.; Desgreniers, S. High Pressure Study of a Highly Energetic Nitrogen-Rich Carbon Nitride, Cyanuric Triazide. *J. Chem. Phys.* **2014**, *141*, 234506. [[CrossRef](#)] [[PubMed](#)]
24. Fabbiani, F.P.; Allan, D.R.; Dawson, A.; David, W.I.; McGregor, P.A.; Oswald, I.D.; Parsons, S.; Pulham, C.R. Pressure-Induced Formation of a Solvate of Paracetamol. *Chem. Commun.* **2003**, *24*, 3004–3005. [[CrossRef](#)] [[PubMed](#)]
25. Fabbiani, F.P.; Allan, D.R.; Marshall, W.G.; Parsons, S.; Pulham, C.R.; Smith, R.I. High-Pressure Recrystallisation—A Route to New Polymorphs and Solvates of Acetamide and Parabanic acid. *J. Cryst. Growth* **2005**, *275*, 185–192. [[CrossRef](#)]
26. Fabbiani, F.P.; Buth, G.; Dittrich, B.; Sowa, H. Pressure-Induced Structural Changes in Wet Vitamin B12. *CrystEngComm* **2010**, *12*, 2541–2550. [[CrossRef](#)]
27. Fabbiani, F.P.; Levendis, D.C.; Buth, G.; Kuhs, W.F.; Shankland, N.; Sowa, H. Searching for Novel Crystal Forms by in situ High-Pressure Crystallisation: The Example of Gabapentin Heptahydrate. *CrystEngComm* **2010**, *12*, 2354–2360. [[CrossRef](#)]

28. Fabbiani, F.P.; Allan, D.R.; Parsons, S.; Pulham, C.R. Exploration of the High-Pressure Behaviour of Polycyclic Aromatic Hydrocarbons: Naphthalene, Phenanthrene and Pyrene. *Acta Crystallogr. Sect. B Struct. Sci.* **2006**, *62*, 826–842. [[CrossRef](#)]
29. Oswald, I.D.; Chataigner, I.; Elphick, S.; Fabbiani, F.P.; Lennie, A.R.; Maddaluno, J.; Marshall, W.G.; Prior, T.J.; Pulham, C.R.; Smith, R.I. Putting Pressure on Elusive Polymorphs and Solvates. *CrystEngComm* **2009**, *11*, 359–366. [[CrossRef](#)]
30. Neumann, M.; Van De Streek, J.; Fabbiani, F.; Hidber, P.; Grassmann, O. Combined Crystal Structure Prediction and High-Pressure Crystallization in Rational Pharmaceutical Polymorph Screening. *Nat. Commun.* **2015**, *6*, 7793. [[CrossRef](#)]
31. Fabbiani, F.P.; Pulham, C.R.; Warren, J.E. A High-Pressure Polymorph of Propionamide from in situ High-Pressure Crystallisation from Solution. *Z. Für Krist. Cryst. Mater.* **2014**, *229*, 667–675. [[CrossRef](#)]
32. Fabbiani, F.P.; Dittrich, B.; Florence, A.J.; Gelbrich, T.; Hursthouse, M.B.; Kuhs, W.F.; Shankland, N.; Sowa, H. Crystal Structures with a Challenge: High-Pressure Crystallisation of Ciprofloxacin Sodium Salts and Their Recovery to Ambient Pressure. *CrystEngComm* **2009**, *11*, 1396–1406. [[CrossRef](#)]
33. Minkov, V.S.; Goryainov, S.V.; Boldyreva, E.V.; Görbitz, C.H. Raman Study of Pressure-Induced Phase Transitions in Crystals of Orthorhombic and Monoclinic Polymorphs of L-Cysteine: Dynamics of the Side Chain. *J. Raman Spectrosc.* **2010**, *41*, 1748–1758. [[CrossRef](#)]
34. Boldyreva, E.; Ivashetskaya, S.; Sowa, H.; Ahsbahs, H.; Weber, H.-P. Effect of High Pressure on Crystalline Glycine: A New High-Pressure Polymorph. *Dokl. Phys. Chem.* **2004**, *396*, 111–114. [[CrossRef](#)]
35. Boldyreva, E.V.; Ivashetskaya, S.N.; Sowa, H.; Ahsbahs, H.; Weber, H.-P. Effect of Hydrostatic Pressure on the γ -Polymorph of Glycine.1. A polymorphic transition into a New δ -Form. *Z. Für Krist. Cryst. Mater.* **2005**, *220*, 50–57. [[CrossRef](#)]
36. Dawson, A.; Allan, D.R.; Belmonte, S.A.; Clark, S.J.; David, W.I.; McGregor, P.A.; Parsons, S.; Pulham, C.R.; Sawyer, L. Effect of High Pressure on the Crystal Structures of Polymorphs of Glycine. *Cryst. Growth Des.* **2005**, *5*, 1415–1427. [[CrossRef](#)]
37. Goryainov, S.; Kolesnik, E.; Boldyreva, E. A Reversible Pressure-Induced Phase Transition in β -Glycine at 0.76 GPa. *Phys. B Condens. Matter* **2005**, *357*, 340–347. [[CrossRef](#)]
38. Fabbiani, F.P.A.; Allan, D.R.; Parsons, S.; Pulham, C.R. An Exploration of the Polymorphism of Piracetam using High Pressure. *CrystEngComm* **2005**, *7*, 179–186. [[CrossRef](#)]
39. Fabbiani, F.P.; Allan, D.R.; David, W.I.; Davidson, A.J.; Lennie, A.R.; Parsons, S.; Pulham, C.R.; Warren, J.E. High-Pressure Studies of Pharmaceuticals: An Exploration of the Behavior of Piracetam. *Cryst. Growth Des.* **2007**, *7*, 1115–1124. [[CrossRef](#)]
40. Prins, L.J.; Reinhoudt, D.N.; Timmerman, P. Noncovalent Synthesis Using Hydrogen Bonding. *Angew. Chem. Int. Ed.* **2001**, *40*, 2382–2426. [[CrossRef](#)]
41. Vippagunta, S.R.; Brittain, H.G.; Grant, D.J. Crystalline solids. *Adv. Drug Deliv. Rev.* **2001**, *48*, 3–26. [[CrossRef](#)]
42. Steiner, T. The Hydrogen Bond in the solid state. *Angew. Chem. Int. Ed.* **2002**, *41*, 48–76. [[CrossRef](#)]
43. Abe, Y.; Harata, K.; Fujiwara, M.; Ohbu, K. Molecular Arrangement and Intermolecular Hydrogen Bonding in Crystals of Methyl 6-O-Acyl-D-Glycopyranosides. *Langmuir* **1996**, *12*, 636–640. [[CrossRef](#)]
44. Boldyreva, E.V. High-Pressure Studies of the Hydrogen Bond Networks in Molecular Crystals. *J. Mol. Struct.* **2004**, *700*, 151–155. [[CrossRef](#)]
45. Boldyreva, E.V. High-pressure Studies of the Anisotropy of Structural Distortion of Molecular Crystals. *J. Mol. Struct.* **2003**, *647*, 159–179. [[CrossRef](#)]
46. Joseph, J.; Jemmis, E.D. Red-, Blue-, or No-Shift in Hydrogen Bonds: A Unified Explanation. *J. Am. Chem. Soc.* **2007**, *129*, 4620–4632. [[CrossRef](#)]
47. Yan, T.T.; Wang, K.; Tan, X.; Liu, J.; Liu, B.B.; Zou, B. Exploration of the Hydrogen-Bonded Energetic Material Carbohydrazide at High Pressures. *J. Phys. Chem. C* **2014**, *118*, 22960–22967. [[CrossRef](#)]
48. Bi, J.; Tao, Y.; Hu, J.; Wang, H.; Zhou, M. High-Pressure Investigations on Urea Hydrogen Peroxide. *Chem. Phys. Lett.* **2022**, *787*, 139230. [[CrossRef](#)]
49. Yan, T.T.; Wang, K.; Tan, X.; Yang, K.; Liu, B.B.; Zou, B. Pressure-Induced Phase Transition in N–H \cdots O Hydrogen-Bonded Molecular Crystal Biurea: Combined Raman Scattering and X-ray Diffraction Study. *J. Phys. Chem. C* **2014**, *118*, 15162–15168. [[CrossRef](#)]
50. Yan, T.T.; Li, S.U.; Wang, K.; Tan, X.; Jiang, Z.M.; Yang, K.; Liu, B.B.; Zou, G.; Zou, B. Pressure-Induced Phase Transition in N–H \cdots O Hydrogen-Bonded Molecular Crystal Oxamide. *J. Phys. Chem. B* **2012**, *116*, 9796–9802. [[CrossRef](#)]
51. Moggach, S.A.; Allan, D.R.; Morrison, C.A.; Parsons, S.; Sawyer, L. Effect of Pressure on the Crystal Structure of L-Serine-I and the Crystal Structure of L-Serine-II at 5.4 Gpa. *Acta Crystallogr. Sect. B Struct. Sci.* **2005**, *61*, 58–68. [[CrossRef](#)] [[PubMed](#)]
52. Boldyreva, E.; Shakhtshneider, T.; Ahsbahs, H.; Sowa, H.; Uchtmann, H. Effect of High Pressure on the Polymorphs of Paracetamol. *J. Therm. Anal. Calorim.* **2002**, *68*, 437–452.
53. Allan, D.; Marshall, W.; Francis, D.; Oswald, I.; Pulham, C.; Spanswick, C. The Crystal Structures of the Low-Temperature and High-Pressure Polymorphs of Nitric Acid. *Dalton Trans.* **2010**, *39*, 3736–3743. [[CrossRef](#)] [[PubMed](#)]
54. Martins, D.M.; Spanswick, C.K.; Middlemiss, D.S.; Abbas, N.; Pulham, C.R.; Morrison, C.A. A New Polymorph of N, N'-Dimethylurea Characterized by X-Ray Diffraction and First-Principles Lattice Dynamics Calculations. *J. Phys. Chem. A* **2009**, *113*, 5998–6003. [[CrossRef](#)] [[PubMed](#)]
55. Munday, L.B.; Chung, P.W.; Rice, B.M.; Solares, S.D. Simulations of High-Pressure Phases in Rdx. *J. Phys. Chem. B* **2011**, *115*, 4378–4386. [[CrossRef](#)] [[PubMed](#)]

56. Oswald, I.D.; Urquhart, A.J. Polymorphism and Polymerisation of Acrylic and Methacrylic Acid at High Pressure. *CrystEngComm* **2011**, *13*, 4503–4507. [[CrossRef](#)]
57. Valkenburg, A.V., Jr. Visual Observations of High Pressure Transitions. *Rev. Sci. Instrum.* **1962**, *33*, 1462. [[CrossRef](#)]
58. Moggach, S.A.; Parsons, S.; Wood, P.A. High-Pressure Polymorphism in Amino Acids. *Cryst. Rev.* **2008**, *14*, 143–184. [[CrossRef](#)]
59. Bassett, W.A. Diamond Anvil Cell, 50th Birthday. *High Press. Res.* **2009**, *29*, 163–186. [[CrossRef](#)]
60. Klotz, S.; Chervin, J.; Munsch, P.; Le Marchand, G. Hydrostatic Limits of 11 Pressure Transmitting Media. *J. Phys. D Appl. Phys.* **2009**, *42*, 075413. [[CrossRef](#)]
61. Mao, H.K.; Xu, J.-A.; Bell, P.M. Calibration of the Ruby Pressure Gauge to 800 Kbar under Quasi-Hydrostatic Conditions. *J. Geophys. Res. Solid Earth* **1986**, *91*, 4673–4676. [[CrossRef](#)]
62. Becker, C.; Dressman, J.; Amidon, G.; Junginger, H.; Kopp, S.; Midha, K.; Shah, V.; Stavchansky, S.; Barends, D. Biowaiver Monographs for Immediate Release Solid Oral Dosage Forms: Pyrazinamide. *J. Pharm. Sci.* **2008**, *97*, 3709–3720. [[CrossRef](#)] [[PubMed](#)]
63. Castro, R.A.; Maria, T.M.; Évora, A.O.; Feiteira, J.C.; Silva, M.R.; Beja, A.M.; Canotilho, J.; Eusébio, M.E.S. A New Insight into Pyrazinamide Polymorphic Forms and Their Thermodynamic Relationships. *Cryst. Growth Des.* **2010**, *10*, 274–282. [[CrossRef](#)]
64. Borba, A.; Albrecht, M.; Gómez-Zavaglia, A.; Suhm, M.A.; Fausto, R. Low Temperature Infrared Spectroscopy Study of Pyrazinamide: From the Isolated Monomer to the Stable Low Temperature Crystalline Phase. *J. Phys. Chem. A* **2010**, *114*, 151–161. [[CrossRef](#)]
65. Tan, X.; Wang, K.; Li, S.U.; Yuan, H.S.; Yan, T.T.; Liu, J.; Yang, K.; Liu, B.B.; Zou, G.T.; Zou, B. Exploration of the Pyrazinamide Polymorphism at High Pressure. *J. Phys. Chem. B* **2012**, *116*, 14441–14450. [[CrossRef](#)]
66. Cherukuvada, S.; Thakuria, R.; Nangia, A. Pyrazinamide Polymorphs: Relative Stability and Vibrational Spectroscopy. *Cryst. Growth Des.* **2010**, *10*, 3931–3941. [[CrossRef](#)]
67. Dreger, Z.A.; Gupta, Y.M. High Pressure Raman Spectroscopy of Single Crystals of Hexahydro-1, 3, 5-Trinitro-1, 3, 5-Triazine (Rdx). *J. Phys. Chem. B* **2007**, *111*, 3893–3903. [[CrossRef](#)]
68. Chieh, P.C.; Subramanian, E.; Trotter, J. Crystal Structure of Malonamide. *J. Chem. Soc.* **1970**, 179–184. [[CrossRef](#)]
69. Nichol, G.S.; Clegg, W. Malonamide: An Orthorhombic Polymorph. *Acta Cryst.* **2005**, *61*, o3427–o3429. [[CrossRef](#)]
70. Nichol, G.S.; Clegg, W. Malonamide: A Tetragonal Polymorph. *Acta Cryst.* **2005**, *61*, o3424–o3426. [[CrossRef](#)]
71. Yan, T.T.; Xi, D.Y.; Ma, Z.N.; Wang, X.; Wang, Q.J.; Li, Q. Pressure-Induced Phase Transition in N–H···O Hydrogen-Bonded Crystalline Malonamide. *RSC Adv.* **2017**, *7*, 22105–22111. [[CrossRef](#)]
72. Jeffrey, G.T.; Maluszynska, H. A Survey of Hydrogen Bond Geometries in the Crystal Structures of Amino Acids. *Int. J. Biol. Macromol* **1982**, *4*, 173–185. [[CrossRef](#)]
73. Watanabe, S.; Abe, Y.; Yoshizaki, R. Tunneling Rotation of Two Inequivalent Methyl Groups in Orthorhombic Acetamide. *J. Phys. Soc. Jpn.* **1986**, *55*, 2400–2409. [[CrossRef](#)]
74. Kang, L.; Wang, K.; Li, S.R.; Li, X.; Zou, B. Pressure-Induced Phase Transition in Hydrogen-Bonded Molecular Crystal Acetamide: Combined Raman Scattering and X-Ray Diffraction Study. *RSC Adv.* **2015**, *5*, 84703–84710. [[CrossRef](#)]
75. Cradwick, P.D. Crystal Structure of the Growth Inhibitor, ‘Maleic Hydrazide’ (1, 2-Dihydropyridazine-3, 6-Dione). *J. Chem. Soc. Perkin Trans.* **1976**, *2*, 1386–1389. [[CrossRef](#)]
76. Katrusiak, A. A New Polymorph of Maleic Hydrazide. *Acta Crystallogr. Sect. C Cryst. Struct. Commun.* **1993**, *49*, 36–39. [[CrossRef](#)]
77. Katrusiak, A. Polymorphism of Maleic Hydrazide. I. *Acta Crystallogr. Sect. B Struct. Sci.* **2001**, *57*, 697–704. [[CrossRef](#)]
78. Wang, K.; Liu, J.; Yang, K.; Liu, B.B.; Zou, B. High-Pressure-Induced Polymorphic Transformation of Maleic Hydrazide. *J. Phys. Chem. C* **2014**, *118*, 8122–8127. [[CrossRef](#)]
79. Ahn, S.; Guo, F.; Kariuki, B.M.; Harris, K.D. Abundant Polymorphism in a System with Multiple Hydrogen-Bonding Opportunities: Oxalyl Dihydrazide. *J. Am. Chem. Soc.* **2006**, *128*, 8441–8452. [[CrossRef](#)]
80. Wen, S.; Beran, G.J. Crystal Polymorphism in Oxalyl Dihydrazide: Is Empirical Dft-D Accurate Enough? *J. Chem. Theory Comput.* **2012**, *8*, 2698–2705. [[CrossRef](#)]
81. Presti, D.; Pedone, A.; Menziani, M.C.; Civalleri, B.; Maschio, L. Oxalyl Dihydrazide Polymorphism: A Periodic Dispersion-Corrected Dft and Mp2 Investigation. *CrystEngComm* **2014**, *16*, 102–109. [[CrossRef](#)]
82. Tan, X.; Wang, K.; Yan, T.T.; Li, X.; Liu, J.; Yang, K.; Liu, B.B.; Zou, G.T.; Zou, B. Discovery of High-Pressure Polymorphs for a Typical Polymorphic System: Oxalyl Dihydrazide. *J. Phys. Chem. C* **2015**, *119*, 10178–10188. [[CrossRef](#)]
83. Jarchow, O.; Kühn, L. Die Kristallstruktur Von A-P-Aminobenzoessäure. *Acta Crystallogr. Sect. B Struct. Crystallogr. Cryst. Chem.* **1968**, *24*, 222–224. [[CrossRef](#)]
84. Banerjee, A.; Agrawal, P.; Gupta, R. Nmr Study of Solid P-Amino Benzoic Acid—Structure and Group Rotation. *J. Prakt. Chem.* **1973**, *315*, 251–257. [[CrossRef](#)]
85. Gracin, S.; Rasmuson, Å.C. Polymorphism and Crystallization of P-Aminobenzoic Acid. *Cryst. Growth Des.* **2004**, *4*, 1013–1023. [[CrossRef](#)]
86. Yang, X.; Wang, X.; Ching, C.B. In Situ Monitoring of Solid-State Transition of P-Aminobenzoic Acid Polymorphs Using Raman Spectroscopy. *J. Raman Spectrosc.* **2009**, *40*, 870–875. [[CrossRef](#)]
87. Yan, T.T.; Wang, K.; Duan, D.F.; Tan, X.; Liu, B.B.; Zou, B. P-Aminobenzoic Acid Polymorphs under High Pressures. *RSC Adv.* **2014**, *4*, 15534–15541. [[CrossRef](#)]
88. Griffiths, P. Crystallographic Data for Cinchomeric Acid and Its Hydrochloride. *Acta Cryst.* **1963**, *16*, 1074. [[CrossRef](#)]

89. Takusagawa, F.; Hirotsu, K.; Shimada, A. The Crystal Structure of Cinchomeric Acid. *Bull. Chem. Soc. Jpn.* **1973**, *46*, 2669–2675. [[CrossRef](#)]
90. Braga, D.; Maini, L.; Fagnano, C.; Taddei, P.; Chierotti, M.R.; Gobetto, R. Polymorphism in Crystalline Cinchomeric Acid. *Chem. Eur. J.* **2007**, *13*, 1222–1230. [[CrossRef](#)]
91. Karabacak, M.; Bilgili, S.; Atac, A. Molecular Structure Investigation of Neutral, Dimer and Anion Forms of 3, 4-Pyridinedicarboxylic Acid: A Combined Experimental and Theoretical Study. *Spectrochim. Acta Part A Mol. Biomol. Spectrosc.* **2015**, *135*, 270–282. [[CrossRef](#)] [[PubMed](#)]
92. Evans, I.R.; Howard, J.A.; Evans, J.S.; Postlethwaite, S.R.; Johnson, M.R. Polymorphism and Hydrogen Bonding in Cinchomeric Acid: A Variable Temperature Experimental and Computational Study. *CrystEngComm* **2008**, *10*, 1404–1409. [[CrossRef](#)]
93. Tong, M.-L.; Wang, J.; Hu, S.; Batten, S.R. A New (3, 4)-Connected Three-Dimensional Anionic Porous Coordination Net Templated by Me₄n⁺ Cations. *Inorg. Chem. Commun.* **2005**, *8*, 48–51. [[CrossRef](#)]
94. Senevirathna, M.; Pitigala, P.; Perera, V.; Tennakone, K. Molecular Rectification: Application in Dye-Sensitized Solar Cells. *Langmuir* **2005**, *21*, 2997–3001. [[CrossRef](#)]
95. Yan, T.T.; Xi, D.Y.; Wang, J.H.; Fan, X.F.; Wan, Y.; Zhang, L.X.; Wang, K. High-Pressure-Induced Phase Transition in Cinchomeric Acid Polycrystalline Form-I. *Chin. Phys. B* **2019**, *28*, 016104. [[CrossRef](#)]
96. Yan, T.T.; Deng, Y.Y.; Yu, Z.Q.; John, E.; Han, R.M.; Yao, Y.; Liu, Y. Exploring the Polymorphism of Cinchomeric Acid at High Pressure. *J. Phys. Chem. C* **2021**, *125*, 8582–8588. [[CrossRef](#)]
97. Yan, T.T.; Xi, D.Y.; Ma, Z.N.; Fan, X.F.; Li, Y. Pressure-Induced Reversible Amorphization in Hydrogen-Bonded Crystalline Phenyl Carbamate Form-I. *J. Phys. Chem. C* **2017**, *121*, 19365–19372. [[CrossRef](#)]